Electronic Supporting Information

{Ni$_{10}$Nb$_{32}$} aggregate: the perspective of isopolyniobates as ligands

Zhijie Liang, Dongdi Zhang, Haiying Wang, Pengtao Ma, Zongfei Yang, Jingyang Niu,* and Jingping Wang*

Henan Key Laboratory of Polyoxometalate Chemistry, Institute of Molecular and Crystal Engineering, College of Chemistry and Chemical Engineering, Henan University, Kaifeng 475004, P. R. China.

CONTENTS

1. Experimental Section

1.1 Materials and Methods

The IR spectra were recorded on a Bruker-Vertex 70 FT-IR spectrometer (used KBr for solid sample palletized) in the range of 400–4000 cm^{-1}. TG analyses were measured by on a Mettler-Toledo TGA/SDTA 851^{e} thermal analyzer in a flowing nitrogen atmosphere with a heating rate of 10 °C·min^{-1}. XRPD experiments were performed on a Bruker AXS D8 Advance diffractometer instrument with Cu Kα radiation (λ = 1.54056 Å) in the 2ϑ = 5–45° range. The solid-state UV/Vis spectra were recorded with a Varian Cary 5000 in the range of 800–190 nm. The mass spectrometer used for the measurements was AB SCIEX Triple TOF 4600. Elemental analyses were performed by using a PerkinEimer Optima 2100DV analyzer. Variable-temperature magnetic susceptibility datas were obtained on Quantum Design MPMS3 magnetometer in the temperature range of 1.8–300 K with an applied field of 1000 Oe.

1.2 X-ray Crystallography

The crystallographic data for **1a** was given in Table S1. Intensity data were collected at 296(2) K on a Bruker APEX-II CCD diffractometer for **1a** using graphite-monochromated Mo Kα radiation (λ = 0.71073 Å). Routine Lorentz and polarization corrections were applied, and an a multi-scan absorption correction was performed using the SADABS program.[S1] The structures of **1a** was solved by direct methods and refined by the full-matrix least-squares method on F^2 using the SHELXL-2008 and SHELXL-2014 program package,[S2] respectively. All hydrogen atoms on water molecules were directly included in the molecular formula. The final refinements include anisotropic thermal parameters of most nonhydrogen atoms, except the disordered K6 atom and few oxygen atoms of the water molecules and the atoms being ADP or NPD if refined anisotropically. ICSD numbers for **1a** are 429933.

Table S1 Crystal data and structure refinement for **1a**.

	1a
Empirical formula	$H_{166}K_{14}Na_6Nb_{32}Ni_{10}O_{183}$
Formula weight	7340.46
T(K)	296.15
Crystal system	Monoclinic
Space group	*I2/m*
a(Å)	15.1399(14)
b(Å)	24.824(2)
c(Å)	25.190(3)
$β$(°)	103.469(2)
V(Å^3)	9206.8(17)

Z	2
Dc(g·cm^{-3})	2.603
Limiting indices	-18≤ h ≤16
	-29≤ k ≤29
	-19≤ l ≤30
μ(mm^{-1})	3.355
GOF on F^2	1.053
$R_1, wR_2[I>2\sigma(I)]$	R_1 = 0.0572
	wR_2 = 0.1330
R_1, wR_2[all data]	R_1 = 0.0893
	wR_2 = 0.1646

1.3 Bond Valence Sum (BVS) Calculations
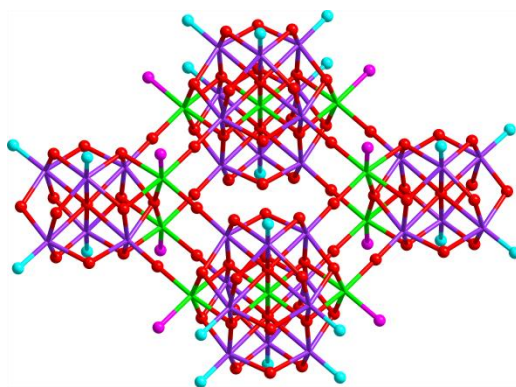
Fig. S1 The location of 8 coordinated water ligands in **1**. The coordinated water ligands in pink.

Table S2 The bond valence sum calculations of all the oxygen atoms in **1**.

Atom	Bond Valence Sum	Atom	Bond Valence Sum	Atom	Bond Valence Sum
O4	1.91	O22	1.76	O26	1.64
O2	1.88	O1	1.73	O28	1.50
O3,O5	1.84	O16,O20	1.72	O33	1.48
O10	1.83	O14,O18,O29	1.71	O25,O32	1.47
O6,O7	1.82	O17	1.70	O27	1.44
O11	1.79	O13, O15	1.68	O24	1.40
O8,O9,O21	1.78	O23	1.67	O31	0.34
O12	1.77	O19	1.66	O30	0.32

$\sum$(O30) = 0.31 -> OH2, $\sum$(O31) = 0.33 -> OH2; Bond valence sum parameters for O(1A), O(2A), O(3A)……O(33A) are the same as O(1), O(2), O(3)……O(33), so they are omitted.

Table S3 Illustration of the oxygen atoms (red, turquoise and pink) in **1**.

Oxygen	Bond Valence Sum
🔴	1.5~2.0
🔵	0.5~1.5
🟣	0.0~0.5

Table S4 The bond valence sum calculations of all the Ni in **1.**

Bond	Bond length	Bond Valence	Valence Sum
Ni(1)−O(1)	2.1594	0.255	
Ni(1)−O(5)	2.032	0.360	
Ni(1)−O(6)	2.023	0.369	Σ(Ni1) = 1.87
Ni(1)−O(9)	2.119	0.285	
Ni(1)−O(12)	2.118	0.285	
Ni(1)−O(30)	2.079	0.317	
Ni(2)−O(2)	2.127	0.278	
Ni(2)−O(3)	2.127	0.278	
Ni(2)−O(4)	1.968	0.428	Σ(Ni2) = 2.02
Ni(2)−O(7)	2.040	0.352	
Ni(2)−O(10)	2.044	0.349	
Ni(2)−O(31)	2.057	0.336	
Ni(3)−O(2)	2.087	0.310	
Ni(3)−O(3)	2.090	0.308	
Ni(3)−O(2)	2.087	0.310	Σ(Ni3) = 1.98
Ni(3)−O(3)	2.090	0.308	
Ni(3)−O(8)	2.015	0.377	
Ni(3)−O(11)	2.027	0.365	

2. Additional Structural Figures
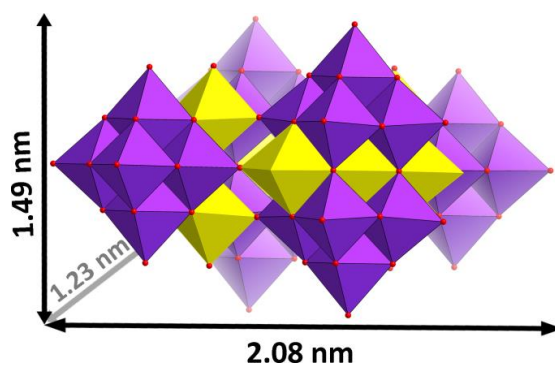
Fig. S2 Polyhedral representation of **1.**
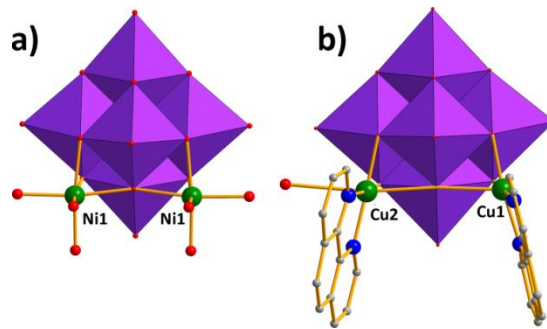
Fig. S3 Combined polyhedral/ball-and-stick representation of subunit **A** (**a**) and {[Cu(L)][Cu(L)(H$_2$O)]Nb$_6$O$_{19}$} (**b**).
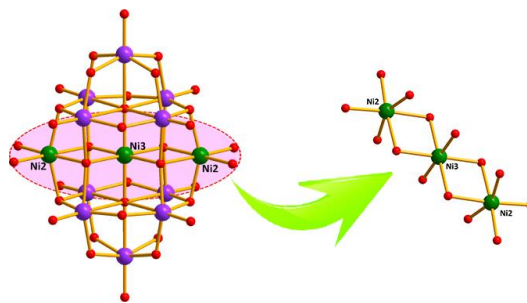
Fig. S4 Ball-and-stick representation of subunit **B** and the coordination of {Ni$_3$}.

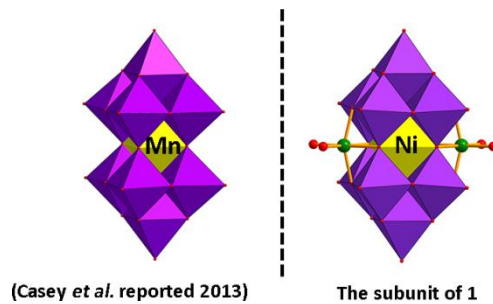(Casey *et al.* reported 2013)   The subunit of 1

Fig. S5 Combined polyhedral/ball-and-stick representation of {MnNb$_{10}$} (left) and B (right).
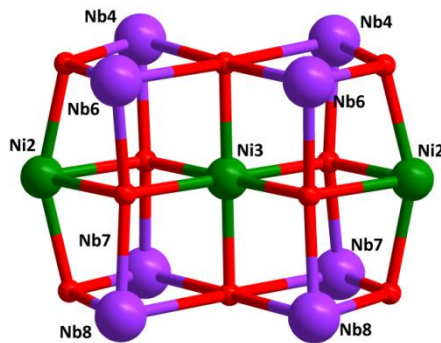
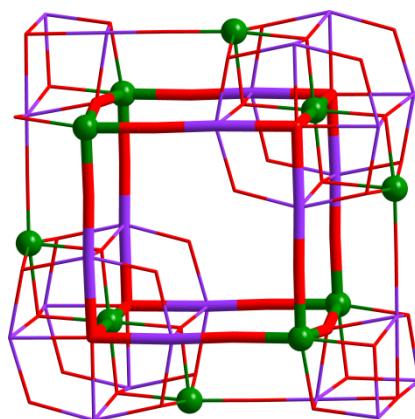**Fig. S6** The model composed of three nickel atoms and eight niobium atoms.

Fig. S7 The cuboid composed of six nickel atoms and others atoms.
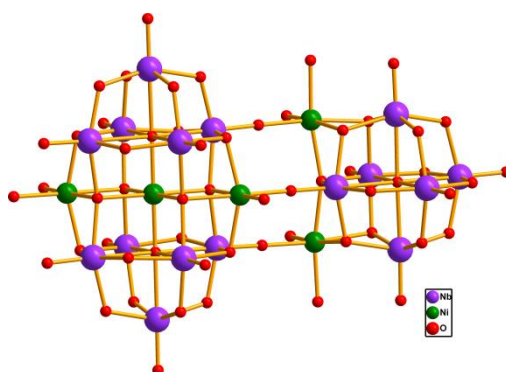
Fig. S8 The ball-and-stick of $\{[Ni_2O_2(H_2O)_2(Nb_6O_{19})][Ni_3(H_2O)_2Nb_{10}O_{33}]\}$.
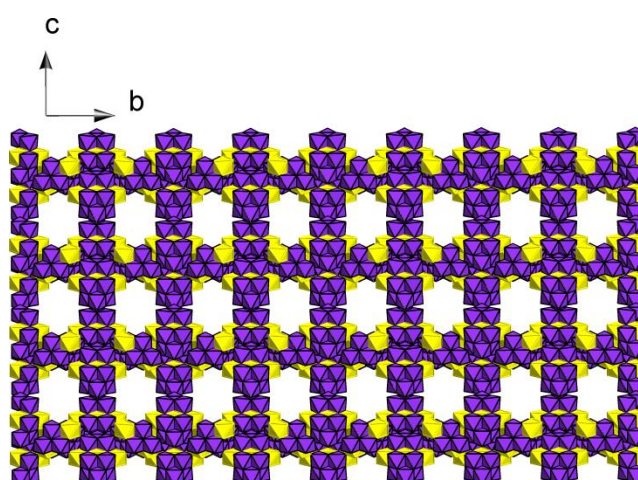
Fig. S9 Solid state packing arrangement of **1a**.
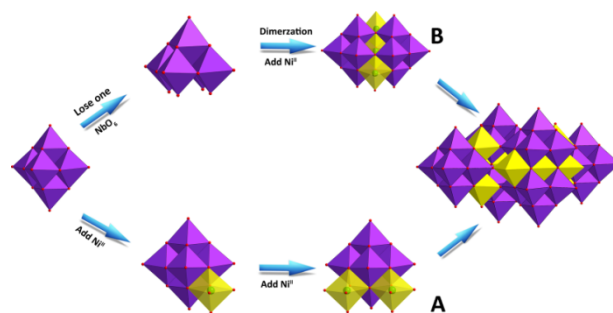
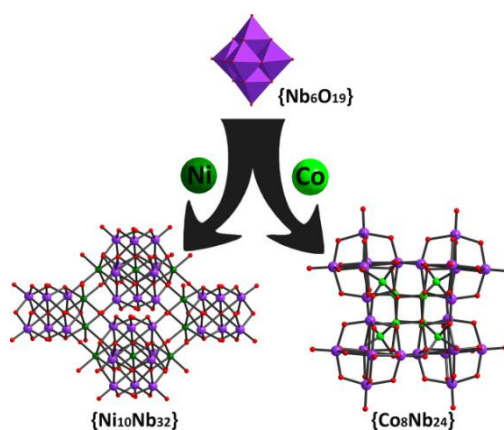**Scheme S1** The postulated steps for the formation of **1**.

Fig. S10 Different metals produce different architectures.

3. Additional measurements

3.1 X-ray powder diffraction (XRPD) spectra

As shown in Fig. S11, the prominent diffraction peaks of experimental pattern match well with the simulated pattern indicating that the samples are pure. However, there are some differences in reflection intensities between them. It may be due to the scanning speed and the variation in preferred orientation and even efflorescence of crystals, which is in accordance with thermogravimetric analysis.
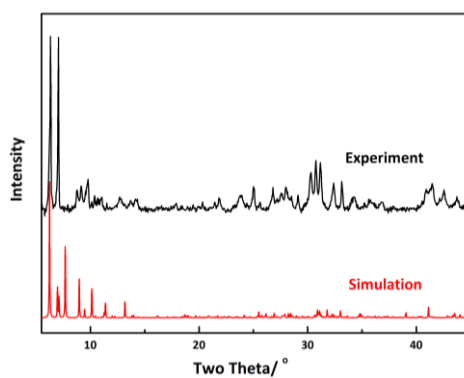
Fig. S11 The PXRD patterns for experiment (top) and simulated (bottom) of **1a**.

3.2 UV-vis spectra

The UV diffuse reflectance spectra of **1a** show three absorption bands in the range 200 to 800 nm. The absorption at 297 nm attribute to oxide-to-metal (O → Nb) charge transfer (OMCT) transitions.[S3] There are two characteristic absorptions at 400 and 700 nm in the visible light region which correspond to $^3A_{2g} \rightarrow {}^3T_{1g}(P)$ and $^3A_{2g} \rightarrow {}^3T_{1g}(F)$ d-d transitions of Ni[II], respectively.[S4]
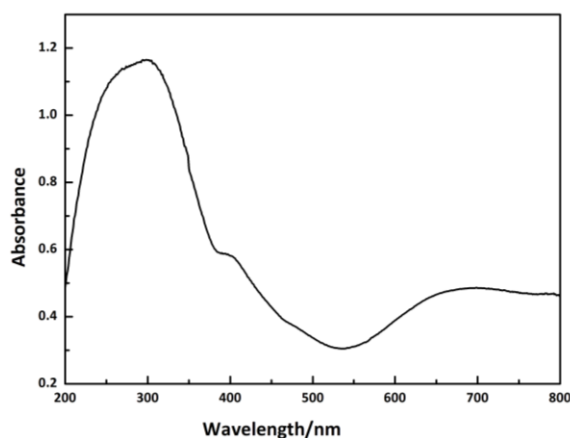

Fig. S12 The UV-vis spectra of **1a** for powdered crystal samples.

3.3 Thermogravimetric analysis

Compound **1a** shows one step of weight loss which can be seen from the Fig. S13. The step of weight loss, giving a total loss of 16.89 % (calcd: 20.35 %), attributed to 73 lattice water molecules, eight coordinated water molecules and four protons (in the form of constitution water molecules) in the range of 25–800 °C. However, there are some deviation between the measured and the theoretical value, owing to the efflorescence of the compound at the room temperature.
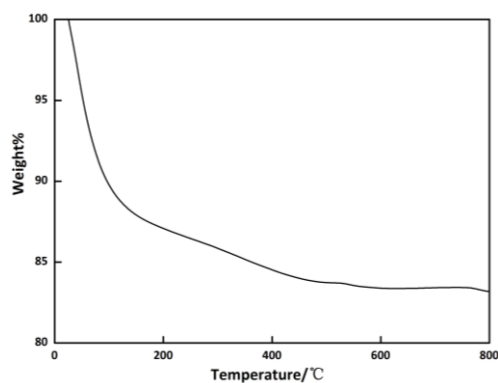
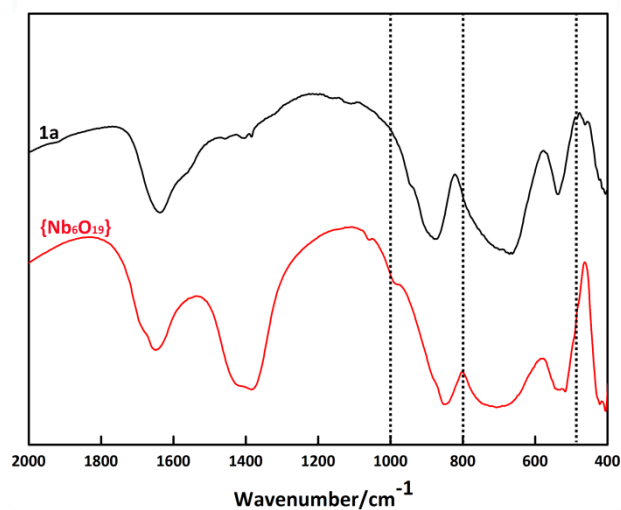

Fig. S13 The TG curve of **1a**.

3.4 IR spectrum

Fig. S14 The comparison of IR curves (**black**: compound **1a**; **red**: $K_7HNb_6O_{19}\cdot13H_2O$).

Table S5 The IR peaks of **1a** and $K_7HNb_6O_{19}\cdot13H_2O$.

	Nb-O_t (cm^{-1})	Nb-O_b-Nb (cm^{-1})
Compound **1a**	872	664, 537
$K_7HNb_6O_{19}\cdot13H_2O$	857	704, 543

4. Magnetism
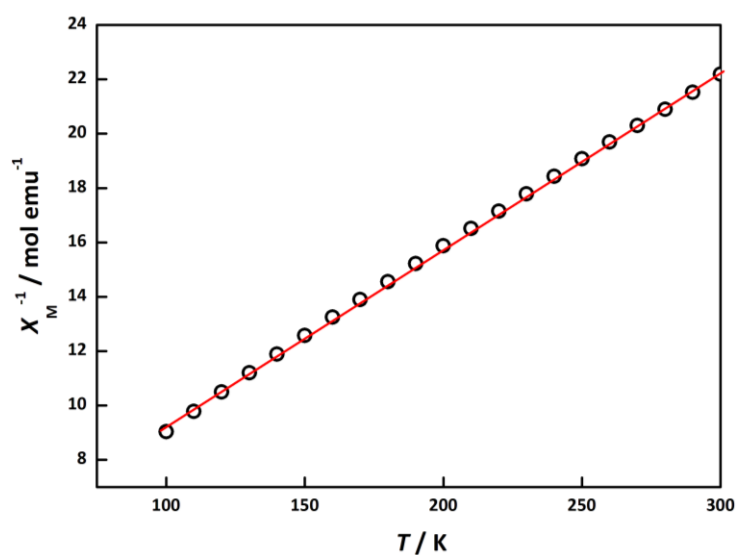
Fig. S15 The plots of $1/\chi_m$ versus T in the range of 100−300 K.

4. Mass spectrometric study of the compound

The following parameters, see Table S6, were consistent for all ESI-MS data collections. This solution was diluted with acetonitrile. Samples were introduced into the MS *via* direct injection at 15 µL/min. The electrospray source was used with the drying nitrogen gas and the ion polarity for all MS data collections recorded was negative.

Table S6 ESI-MS parameters used in each data acquisition.

MS Parameter	Setting during data collection
Mass Range (m/z)	100-3000
Collision Energy (V)	-5
Transfer time (min)	5
Time of Acquisition (min)	2
Temperture (°C)	0
Declustering potential (V)	-10
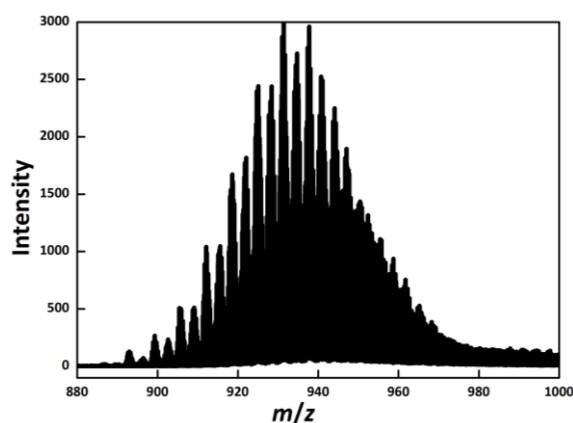
Fig. S16 Extension of the peak at *m/z* 931.4.
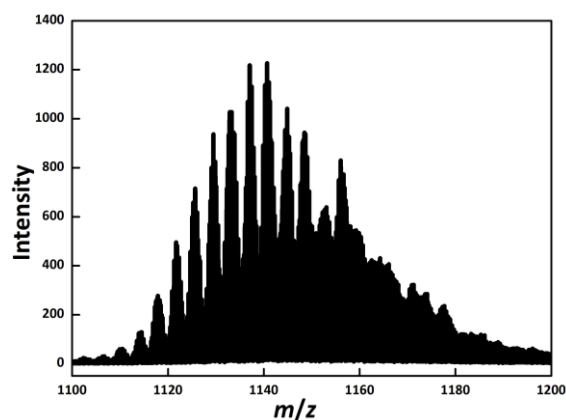
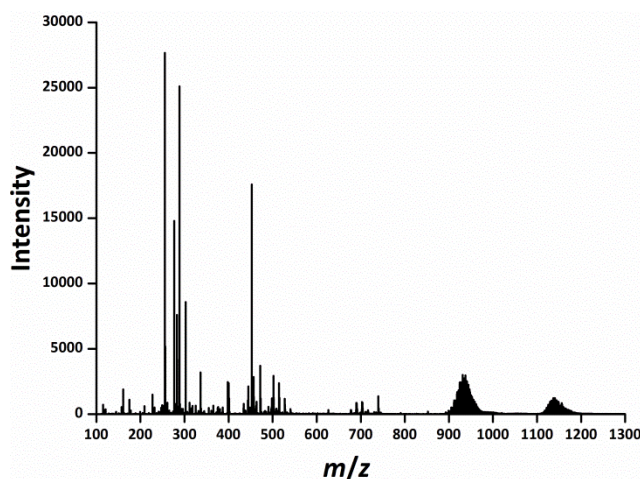**Fig. S17** Extension of the peak at *m/z* 1140.7.

Fig. S20 ESI-MS of **1a** in water-acetonitrile mixtures (the overall scale).

Table S8 The other assignment of mass spectral data for compound **1a**.

m/z (obs.)	Peaks Assignment	m/z (calc.)
498.37	$[K_7HNi_3Nb_{10}O_{34}(H_2O)_4]^{4-}$	498.97
501.97	$[K_8NaNi_2Nb_6O_{23}(H_2O)_7]^{3-}$	501.56
508.61	$[K_7NaNi_3Nb_{10}O_{34}(H_2O)_5]^{4-}$	508.97
514.62	$[K_7Na_2Ni_2Nb_6O_{23}(H_2O)_{10}]^{3-}$	514.21
677.81	$[K_7H_2Ni_3Nb_{10}O_{34}(H_2O)_6]^{3-}$	677.64
685.14	$[K_9Ni_3Nb_{10}O_{34}(H_2O)_3]^{3-}$	685.02
690.13	$[K_8HNi_3Nb_{10}O_{34}(H_2O)_6]^{3-}$	690.33
698.46	$[K_7Na_2Ni_3Nb_{10}O_{34}(H_2O)_7]^{3-}$	698.30
703.11	$[K_9Ni_3Nb_{10}O_{34}(H_2O)_6]^{3-}$	703.03

5. References

S1. G. M. Sheldrick, *SADABS, Bruker–Siemens Area Detector Absorption and Other Correction*, Version 2008/1, Bruker: Madison, WI, 2008.

S2. (a) G. M. Sheldrick, *Acta. Crystallogr. Sect. A,* 2008, **64**, 112; (b) P. Müller, *Crystal structure refinement: a crystallographers guide to SHELXL*. Oxford University Press: Oxford, 2006.

S3. A. V. Besserguenev, M. H. Dickman and M. T. Pope, *Inorg. Chem.,* 2001, **40**, 2582.

S4. F. A. Cotton, G. Wilkinson, C. A. Murillo and M. Bochmann, *Advanced Inorganic Chemistry,* Wiley Interscience, New York, 6th edn, 1999.